Available online at www.sciencedirect.com

ScienceDirect

Procedia CIRP 136 (2025) 787–791

www.elsevier.com/locate/procedia

35th CIRP Design 2025

Development and implementation of a manipulator for the automated handling of electrodes during the disassembly of lithium-ion pouch cells

Sebastian Henschel*, Simon Buschulte, Florian Kößler, Jürgen Fleischer

wbk – Insitute of Production Science at Karlsruhe Institute of Technology KIT, Kaiserstraße 12, 76131 Karlsruhe, Germany

* Corresponding author. Tel.: +49 1523 950 2568; *E-mail address:* sebastian.henschel@kit.edu

Abstract

Lithium-ion batteries, driven by the increasing production of electric vehicles, have seen a significant rise in demand, especially space efficient pouch cells. Current disassembly methods for individual battery cells are either non-existent or involve a high degree of manual labor. This research aims to develop a manipulator unit to automate the disassembly of lithium-ion pouch cells, enabling efficient recycling of their components. The main challenge lies in handling thin, flexible electrodes that adhere to each other due to the electrolyte. A gripper and hold-down device will be developed and tested to support automated serial disassembly.

Keywords: Battery; e-Mobility; Recycling

1. Motivation

Scarce natural resources as well as geopolitical problems in sourcing are amongst the many factors, leading to a larger focus on lithium-ion battery recycling in recent years. This is further supported by raw material being the largest cost driver in cell production as well as new EU legislation. [1,2]

Current industrial scale recycling setups are focused on the pyro- or hydrometallurgical approach, which involve manual disassembly steps to dismantle the battery pack up to a certain level. For the hydrometallurgical route, material is then ground up and fed into a process route involving several acids and bases to recover the elementary materials such as Nickel and Cobalt salts. When choosing pyrometallurgy, the individual cells or even entire battery modules are added to a smelting furnace resulting in the burning of organic material while recovering certain metals in their liquid form. Other material, such as the Lithium is bound in the slack, which can be further processed, resulting in a combination of the pyrometallurgic and hydrometallurgical approach [3,4].

Due to the large demands in energy or chemicals, a third route is becoming more and more interesting [5–7]. The direct recycling aims to recover a larger share of battery materials and also collect them in their molecular state, without dissolving them down into individual elements. This is especially interesting for production scrap, which is obtained during cell manufacturing in different forms. While an exact quantification of scrap rates is difficult, it is estimated that production scrap will be the dominant source of secondary battery material until at least 2030 [8].

In current research for the direct recycling, a primary focus is set on the cathode and anode active material, as it contains the most precious raw material. The process engineering methods currently being developed largely benefit from a separated and clean material input stream. It is therefore often advantageous to separate the material down to the individual cell component level [9–11]. As most direct recycling approaches are still in the laboratory or research phase, the dismantling of individual cells is a predominantly manual process involving the opening and consequently separation of

10.1016/j.procir.2025.08.134

anodes, cathodes and separator material. However, first recycling companies are also applying the manual cell opening and disassembly at a larger scale, in order to produce higher quality black mass to be then further processed in a hydrometallurgical route.

Due to the very time-consuming process of manually separating the different electrodes, as well as the potential health hazards posed by evaporating solvents from the cell-electrolyte or possible hydrogen fluoride (HF) formation, the automatization of the cell disassembly process seems mandatory for a large-scale application of the direct recycling process, as was shown by the authors in [12]. This paper describes the general concept for such an automated cell disassembly as well as first developed manipulator units, and their interaction with the electrode sheets.

2. Approach

Due to the large number of different cell formats, cell designs and other distinctions currently on the market, a modular setup is chosen for the automated disassembly of the individual battery cells. This allows for simple adaptations to future changes in requirements as well as the incorporation of new processing technology. Following the modular approach, different process steps are divided amongst separate production modules. One module is responsible for the opening of pouch cells and removal of the cell casing, a separate module is to perform the unstacking of single-sheet or z-folded cell stacks. By introducing a second cell-opening module, tailored to prismatic cell casings, z-folded cells inside a prismatic casing could also be processed using the presented system, showing the flexibility of the modular approach.

Up to three production modules are to be incorporated into a common microenvironment, which provides a carefully controlled climatic condition for the processes happening within. This process of capsulating individual operations, has already been applied successfully to the flexible battery cell production as shown in [13–17]. In the context of battery cell disassembly, the microenvironments can serve two main purposes. On the one hand they serve as a protective environment for the recycled product, eliminating possible environmental contamination such as dust or other impurities. Simultaneously, the microenvironments also protect employees from the harmful substances emitted from the cell disassembly process. The different disassembly modules are incorporated into the microenvironments via zero-point-clamping systems, allowing for a fast and easy reconfiguration if necessary. This adaptability is further enhanced, by individual PLCs, present in each disassembly module and a central command unit associated with each microenvironment.

Due to the lack of existing automation, the material properties of end-of-life battery cell stacks and components such as electrodes or separators are largely unknown. In the same way, necessary process forces to separate the cell components from one another are not yet quantified. Manual disassembly practices have shown, that due to the compression during cell operation, as well as the wetting with electrolyte, adhesion between the different layers can be observed. In order to quantify this adhesion, as well as to develop an understanding as to what influences this behavior, a semiautomated disassembly setup has been developed. It was used to test different manipulator units as a first step. Therefore, transferable forces of different units were measured for both individual electrodes, as well as separator sheets.

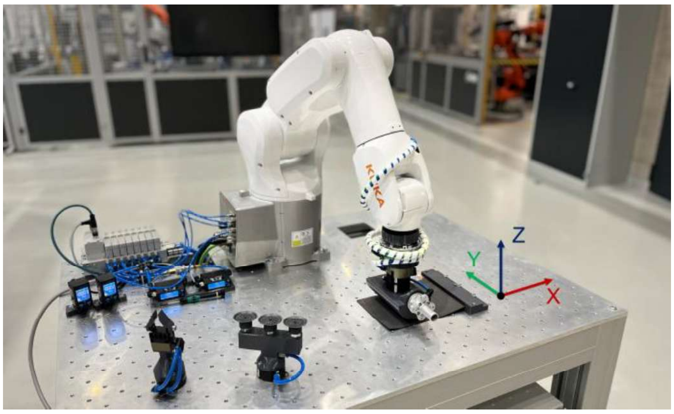

Fig. 1. The semi-automated disassembly setup has a universal kinematic and a six-axis force-torque sensor as main components. The chosen stationary frame of reference is shown as a coordinate system.

3. Experimental

The semi-automated disassembly setup consists of a *Kuka KR4-R600* robotic actuator capable of performing simple peel tests, as well as more complex separation operations, and can be seen in fig.1. It is equipped with a six-axis force-torque sensor *ForTTran SG 500-20* for the measurement of the existing forces. It captures forces up to 500 N in X and Y, as well as 900 N in Z direction, with an accuracy of 0.1 N. The sensor data is transferred to the Kuka native Robot-Sensor-Interface (RSI) with a sampling frequency of 250 Hz for easy combination of sensor datapoints with the corresponding robot pose in form of six axis angles. The combined dataset is continuously streamed to a connected workstation via UDP, which then transforms the measured force values using quaternions, so that a stationary frame of reference is given (see fig.1). For easier visualization, noise removal for the resultant data stream was carried out, using a 5-point FFT filter.

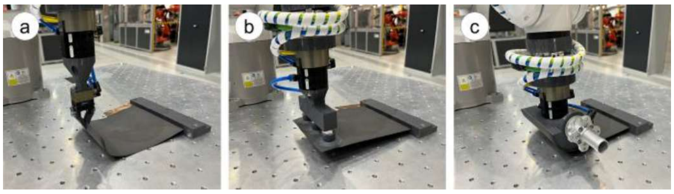

Fig. 2. Three concepts were chosen to further analyze their ability to handle cell components. These include the two-finger gripper (a), the suction cup gripper (b) and the low-pressure gripper (c).

In preliminary handling tests, different suction cups are manually placed on anode material and the air is evacuated. After removing the suction cups, the area on the anode is assessed for damage. Following this initial assessment, a utility analysis was carried out, for different gripping concepts and configurations. The three most promising concepts were then designed and further tested, as can be seen in fig. 2. These include a suction cup gripper with three *Schmalz SFF 40*

EPDM-45 G1/4-AG suction cups that are installed on a 3D-printed mount. The low-pressure air for the suction-cup gripper is supplied by a *Schmalz SEG 10 HS* ejector. The main body of the two-finger gripper (*MPG-plus 32*) is produced by *Schunk*, with a custom 3D-printed finger design with a surface area of 185 mm^2 for each finger.

As a third option, a 3D-printed low-pressure gripper in the form of a sectorial vacuum suction roller was investigated, which uses a *Schmalz SCG 1xE100 A MA AR* ejector as a low-pressure supply. The design of a half cylinder for the third gripper was chosen, so that the gripped sheet can fully enclose the active gripping surface, reducing the amount of air leakage.

For the analysis of the maximum transferrable forces between robotic manipulator and the different cell components graphite anodes produced by *EnerTech* with a thickness of 105,5 µm, as well as *Celgard* separators were tested. The separator has a PP/PE/PP sandwich structure with a thickness of 20 µm.

The first tests are conducted with a single sheet laid flat on a surface and clamped down on one side, as can be seen in fig. 2. Each of the three grippers is attached to the loose end of the sheet and moved in the positive Z-direction by the robotic arm (see fig. 1 for frame of reference). During the movement the maximum forces applied are recorded, either until the gripper detaches from the sheet or the sheet starts tearing apart. After ten repetitions, the average maximum value for each gripper is calculated. Further testing with the suction cup gripper moving parallel to the sheets' surface was conducted to examine the behavior during different pulling orientations.

In a second step, different concepts for the fixation of the cell stack during the disassembly process were analyzed, as can be seen in fig. 3. One concept uses a perforated plate with a chamber underneath that can be evacuated using the SCG ejector. When a cell stack is placed on the plate a vacuum can be created and thus the stack is held down across the whole surface. A second concept uses the same suction cups that were chosen for the gripper. To fixate the cell stack, this design uses four suction cups that are placed on a plate with holes accommodating the suction cups. The suction cups are mounted facing up and flush with the plate and evacuated using two SEG ejectors. Then similar to the tests performed with the gripper designs, each concept's maximum holding force was tested. For these tests the suction cup gripper was used, due to it achieving the highest maximum forces and therefore reducing the possibility of being the bottleneck in testing the concepts for fixation. The maximum forces for each experimental setup were recorded for 10 repetitions.

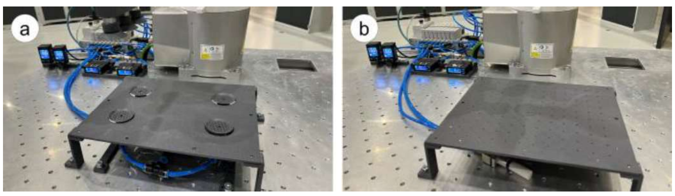

Fig. 3. Different concepts for the cell stack fixation were analyzed. These include a suction cup approach (a) and a low-pressure holding fixture (b).

After determining the most suitable manipulator, it was used for first disassembly tests. These were conducted using a substitute battery-cell system. The aforementioned cell materials were stacked using an automated single-sheet stacking operation. The resulting cell stack was taped, contacted and packaged in pouch foil. 99.5% isopropyl alcohol was used as an electrolyte replacement and the operating pressures of a battery lifecycle were simulated using a 25ton hydraulic press.

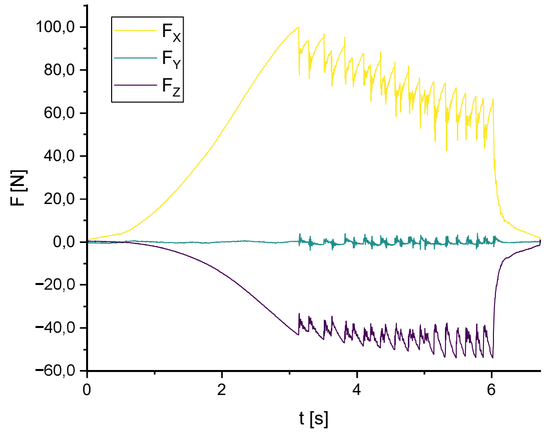

Fig. 4. Due to the one-sided fixation of the test material, forces both in X as well as in Z Direction can be observed. The given example of a suction cup gripper on anode material shows the much larger existing force in the X direction as well as the typical slide-and-stick behavior of the suction cups.

4. Results

Suction cup designs with large inner diameters or deep cups were dismissed in the preliminary test, due to the thin anode material being deformed and, in some cases, even delaminated, once the vacuum is activated. Therefore, designs with large, flat cups are recommended for the handling of thin cell components and were used in all further experiments of this paper.

A typical graph containing the forces in all three spatial dimensions can be seen in fig. 4. It is clearly visible, that the one-sided fixation of the material leads to a resultant force in both the X- and the Z-direction. Another visible phenomenon is the slide-and-stick behavior of the suction cup on the anode material. The repeated loss of suction on the porous material surface is followed by the regain of control, shown by the individual peaks of the recorded force in both X- and Z-direction.

It is notable at this point, that even with the aforementioned effects taken into consideration, the results of the experiments were highly repeatable. Fig. 5 depicts the recorded force values in Z-direction for all repetitions of a setup using the two-finger gripper and anode material.

It is clearly visible, that both the maximum exerted force, as well as the progression are highly similar between the different experiments. This is further shown by small standard deviations across the repetitions.

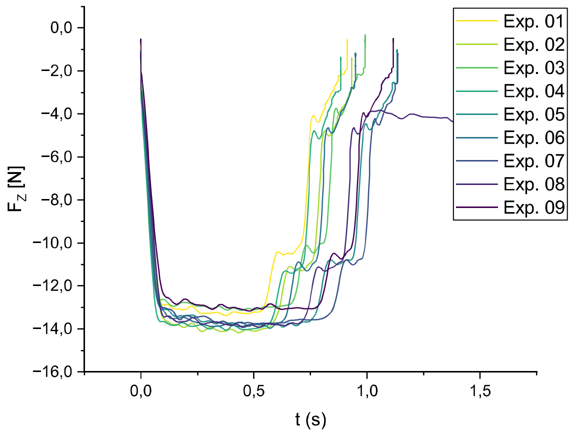

Fig. 5. The maximum transferable process forces for the two-finger gripper handling anode sheets are highly repeatable and peak at around 8,0N.

For the vertical pulling tests using an anode, the suction cup gripper performed the best with average maximum forces of 99,5 N and 44,9 N in x- and z-direction, respectively, as can be seen in table 1. The second-best option with 9,1 N and 14,2 N in x- and z-direction is the finger gripper, while the low-pressure gripper performed the worst with 10,3 N and 3,1 N in x- and z-direction. Due to the low gripping force and higher relative standard deviations compared to the other gripper designs, the low-pressure gripper was excluded from further testing.

Table 1. Maximum forces recorded for different gripper and material combinations and calculated standard deviations for the X- and Z- direction. SC = suction cup gripper; FG = finger gripper; LP = low-pressure gripper.

Experiment	Ø F_{X_max} [N]	Ø F_{Z_max} [N]	σ_X [N]	σ_Z [N]
SC Anode vertical	99,5	44,9	3,5	3,6
FG Anode vertical	9,1	14,2	0,2	0,4
LP Anode vertical	10,3	3,1	2,1	0,2
SC Separator vertical	38,7	19,6	1,0	0,6
FG Separator vertical	17,7	22,0	1,7	1,0
SC Separator diagonal	50,7	18,4	0,6	2,4

The graphs in Fig. 6 show the total force amplitudes calculated from the X- and Z- values of different manipulators and material combinations over the Z-displacement of the gripper. It should be noted that the maximum force in X-direction does not necessarily occur at the same time as the maximum force in Z-direction. Therefore, this visualization should be used to evaluate the differences between different manipulators rather than for the exact force values.

The suction cup gripper achieved the highest total force while testing on an anode by a significant margin. The second highest values were reached by the finger gripper at the end of the measuring interval, just before the fingers slipped off the Anode. The lowest values were achieved by the low-pressure gripper. The oscillation of the low-pressure gripper curve can be explained by the same stick-slip-behavior that was previously described for the suction-cup gripper. In this case the slipping and reattaching happened in smaller increments, but with a higher frequency compared to the suction-cup gripper. Both the suction cup gripper and the finger gripper achieved similar total maximum forces while testing on a separator.

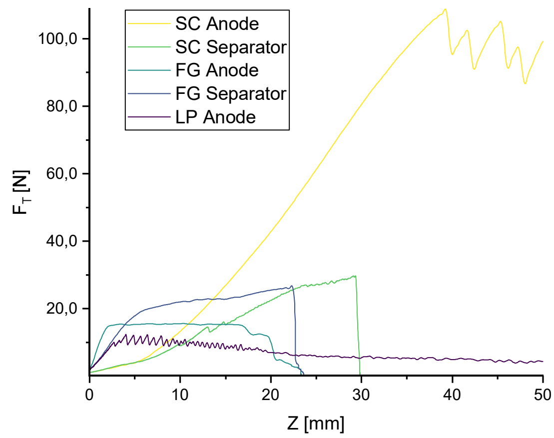

Fig. 6. Exemplary force-distance curves for different manipulator units and materials. The suction cup gripper can transfer up to 8 times more force compared to the alternatives. SC = suction cup gripper; FG = finger gripper; LP = low-pressure gripper.

Table 2 shows the received maximum forces for the different cell stack fixtures considered in this paper. While the low-pressure fixture is able to transmit larger forces for both the anode and separator material, it also has a much larger standard deviation, relative to the achieved forces.

Table 2. Maximum forces recorded for the suction-cup holding fixture (SCF) and low-pressure holding fixture (LPF) and material combinations and calculated standard deviations for the z- direction.

Experiment	Ø F_{z_max} [N]	σ_Z [N]
SCF Anode vertical	63,7	1,5
LPF Anode vertical	67,3	7,1
SCF Separator vertical	18,7	1,8
LPF Separator vertical	57,4	8,7

5. Discussion

Both the suction cup gripper as well as the finger gripper have shown high repeatability of the achieved forces during testing. Even though the finger gripper didn't reach forces as high as the suction cup gripper it can still be seen as a viable option for the automated cell disassembly. However, due to the much simpler and faster positioning of the suction-cup gripper and therefore lower achievable cycle times it should be prioritized for further testing.

Comparing the vertical and diagonal test results of the suction-cup gripper with separator material, it can be seen that the pose of the suction cup gripper relative to the sheet has a significant impact on the maximum transferred force. This therefore has to be considered, when planning the trajectory for the final application.

To improve the reliable layer separation during first disassembly tests, fingers were added to the holding fixture that clamp down the second sheet from the top. This improved separation significantly and thus the design should be refined and implemented in future versions. The holding fixture with four suction cups is sufficient to reliably keep the cell stack from shifting. Thus, it should be the preferred choice over the low-pressure fixture, which is also more prone to loss of holding force from imprecise cell stack placement. While conducting these tests additional isopropyl alcohol was added to the stack to simulate strong adhesion between layers. While the separation of anodes worked without a problem, the suction-cup gripper struggled in some scenarios to fully remove the separator. This can most likely be remedied by adding an additional suction cup to the gripper. Since separate grippers for anodes, cathodes and separator will be required to avoid cross-contamination, the implementation of gripper designs with a different number of suction cups is not an issue.

6. Conclusion and Outlook

In this paper, the concept for a modular automated lithium-ion battery cell disassembly has been presented. It is based upon individual production modules, placed into a microenvironment, thus protecting both the recycled material and factory employees. As a first step, different manipulator units for the handling of individual cell components, such as anodes or separator sheets have been developed. They were tested according to their maximum transmitted forces and the suction cup gripper proved to be the most reliable solution. The same was done for different cell stack fixtures. Once again, the suction cup solution was most reliable and is therefore favored for future implementation.

As a next step, the now proven manipulating principles for the automated cell disassembly will have to be tested on real end-of-life cells. By doing so the requirements for a fully automated system can be quantified. At the same time, further investigation into the disassembly strategy, in terms of necessary trajectories and used manipulators is required as can be seen in fig. 7. This knowledge can then be transferred into the design of an automated setup for the disassembly of stacked lithium-ion cells.

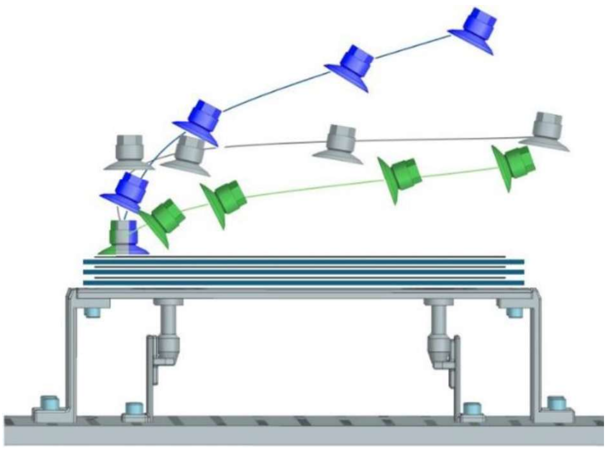

Fig. 7. Illustration of possible 2D-trajectories, which could be used for the cell stack separation.

Acknowledgements

The authors thank the German Ministry of Education and Research (BMBF) for funding the project *DiRecReg* (03XP0553C). This work contributes to the research performed at *KIT-BATEC* (KIT Battery Technology Center) and at *CELEST* (Center for Electrochemical Energy Storage Ulm Karlsruhe).

References

[1] G. Harper, R. Sommerville, E. Kendrick, L. Driscoll, P. Slater, R. Stolkin, A. Walton, P. Christensen, O. Heidrich, S. Lambert, A. Abbott, K. Ryder, L. Gaines, P. Anderson, Recycling lithium-ion batteries from electric vehicles, Nature 575 (2019) 75–86.

[2] S. Orangi, N. Manjong, D.P. Clos, L. Usai, O.S. Burheim, A.H. Strømman, Historical and prospective lithium-ion battery cost trajectories from a bottom-up production modeling perspective, J. Energy Storage 76 (2024) 109800.

[3] V. Gupta, X. Yu, H. Gao, C. Brooks, W. Li, Z. Chen, Scalable Direct Recycling of Cathode Black Mass from Spent Lithium-Ion Batteries, Adv. Energy Mater. 13 (2023) 2203093.

[4] C.P. Makwarimba, M. Tang, Y. Peng, S. Lu, L. Zheng, Z. Zhao, A. Zhen, Assessment of recycling methods and processes for lithium-ion batteries, iScience 25 (2022) 104321.

[5] E. Kallitsis, A. Korre, G.H. Kelsall, Life cycle assessment of recycling options for automotive Li-ion battery packs, J. Clean. Prod. 371 (2022) 133636.

[6] L. Kurz, S. Forster, R. Wörner, F. Reichert, Environmental Impacts of Specific Recyclates in European Battery Regulatory-Compliant Lithium-Ion Cell Manufacturing, Sustainability 15 (2022) 103.

[7] K. Lin, M. Lin, J. Ruan, Occupational Threat of Recycling Spent Lithium-Ion Batteries by Vacuum Reduction, ACS Sustain. Chem. Eng. 10 (2022) 15297–15304.

[8] The Lithium-Ion (EV) battery market and supply chain - Market drivers and emerging supply chain risks, Roland Berger, 2022.

[9] T. Yildiz, P. Wiechers, H. Nirschl, M. Gleiß, Direct recycling of carbon black and graphite from an aqueous anode slurry of lithium-ion batteries by centrifugal fractionation, Energy 2 (2024) 100082.

[10] P. Zhu, E.H. Driscoll, B. Dong, R. Sommerville, A. Zorin, P.R. Slater, E. Kendrick, Direct reuse of aluminium and copper current collectors from spent lithium-ion batteries, Green Chem. 25 (2023) 3503–3514.

[11] J. Ma, J. Wang, K. Jia, Z. Liang, G. Ji, Z. Zhuang, G. Zhou, H.-M. Cheng, Adaptable Eutectic Salt for the Direct Recycling of Highly Degraded Layer Cathodes, J. Am. Chem. Soc. 144 (2022) 20306–20314.

[12] S. Henschel, P.-T. Dörner, F. Kößler, J. Fleischer, Mechanische Zelldemontage für das direkte Recycling/Mechanical battery cell disassembly for direct end-of-life battery recycling, Wt Werkstattstech. Online 113 (2023) 278–281.

[13] J. Fleischer, F. Fraider, F. Kößler, D. Mayer, F. Wirth, Agile Production Systems for Electric Mobility, Procedia CIRP 107 (2022) 1251–1256.

[14] S. Henschel, K. Hubalek, N. Neub, F. Kößler, J. Fleischer, Implementation of an Agile Manufacturing System for the Lithium-Ion-Cell-Production based on Individual Microenvironments, Procedia CIRP 130C (2024) 619–624.

[15] S. Henschel, N. Schmidgruber, S. Schabel, F. Kößler, D. Mayer, J. Fleischer, Cost Modell for Agile Battery Cell Manufacturing, in: 2024 1st Int. Conf. Prod. Technol. Syst. E-Mobil. EPTS, IEEE, Bamberg, Germany, 2024: pp. 1–6.

[16] S. Henschel, F. Kößler, J. Fleischer, Material Flow of an Agile Battery Cell Production System Based on Diffusion-Tight Transport Boxes and Driverless Transport Systems, in: T. Bauernhansl, A. Verl, M. Liewald, H.-C. Möhring (Eds.), Prod. Lead. Edge Technol., Springer Nature Switzerland, Cham, 2024: pp. 550–558.

[17] F. Kößler, D. Mayer, J. Fleischer, Agile Produktionssysteme in der Batteriezellfertigung/Plant Concept for Highly Automated and Agile Calendering of Battery Electrodes, Wt Werkstattstech. Online 112 (2022) 492–495.